European Journal of Radiology Open 8 (2021) 100347

Contents lists available at ScienceDirect

European Journal of Radiology Open

journal homepage: www.elsevier.com/locate/ejro

Diagnostic accuracy of the attenuation value in abdominal contrast enhanced dynamic multi-detector-row computed tomography for esophageal varices in patients with liver cirrhosis

Yasuhiro Inokuchi *, Masahiro Uematsu, Tsuneyuki Takashina

Department of Radiology, Edogawa Hospital, Edogawaku, Tokyo, 133-0052, Japan

ARTICLE INFO

Keywords:
Liver cirrhosis
Esophageal and gastric varices
Multidetector computed tomography
Contrast media

ABSTRACT

Purpose: To investigate whether the attenuation value obtained by subtracting the CT value obtained from abdominal dynamic contrast enhanced (ADCE)-MDCT imaging of the equilibrium phase from the value obtained from that of the portal phase in hepatic parenchyma is useful in distinguishing normal liver from liver cirrhosis (LC) and to predict the development of esophageal varices (EVs) in patients with LC.

Materials and methods: We assigned 72 outpatients to group A (n = 45; normal liver) and group B (n = 27; LC), who underwent ADCE-MDCT. The attenuation value and CT value of the hepatic parenchymal portal and equilibrium phase were compared, and the correlation between attenuation value and biomarkers (ALB, T-bil, PLT, FIB-4, APRI, and AAR) was investigated. Furthermore, we investigated differences in the attenuation value, FIB-4, APRI, and AAR between the two subgroups of group B [without EVs (group a) and with EVs (group b)]. We performed receiver operating characteristic (ROC) analysis of the attenuation value, FIB-4, APRI, and, AAR for subgroup a vs b and evaluated the diagnostic accuracy.

Results: Significant differences were observed between groups A and B in all items. The attenuation value correlated with ALB, T-bil, PLT, FIB-4, and APRI. Only attenuation value showed a significant difference between groups a and b. The best cut-off attenuation value, FIB-4, APRI, and AAR for predicting EVs, according to ROC analysis was 13.4 HU, 6.8, 1.9, and 1.5.

Conclusions: Attenuation value can be useful to quantitatively classify normal liver and LC and to predict EVs in patients with LC.

1. Introduction

Liver cirrhosis (LC) is associated with various complications, which have significant effects on the prognosis of patients. Portal hypertension is regarded as the primary complication of LC, and it is known to cause the formation of esophageal varices (EVs). The development of EVs is a serious condition in the context of LC, as bleeding from varices is often life-threatening for patients with LC [1–4]. The guidelines recommend screening for EVs at the time of diagnosis in patients with LC. Even if EVs are undetected, repeat endoscopy should be performed every 1–3 years in patients with LC [5]. Endoscopic examinations are invasive procedures; repeated endoscopies have several side effects including perforation and aspiration [6]. In addition, it is also not cost effective due to the lack of actual detection of varices in many patients [7]. Thus, the accurate and non-invasive techniques to predict the development of EVs are always much awaited before endoscopic examinations and they might be able to decrease unneeded endoscopic examinations. The mechanism of EV development is considered to involve increased blood flow resistance in combination with severe hepatic fibrosis [4,8–12]. An understanding of intrahepatic hemodynamics is important for evaluating the development of EVs. Abdominal dynamic contrast enhanced multi-detector-row computed tomography (ADCE-MDCT) is known to have utility for identifying the occurrence of hepatocellular carcinoma, changes in gross morphology of the liver and determining the presence or absence of portal vein thrombosis and EVs. Moreover, it is also useful to investigate hemodynamics [13–15]. In a normal liver, some of the in-flowed contrast medium leaks into the hepatic extracellular space (ECS) according to the concentration gradient and remaining flows through the hepatic sinusoid and out into the hepatic vein [16,17]. However, when hepatocytes are damaged and fibrous tissue is formed

* Corresponding author at: Department of Radiology, Edogawa Hospital, 2-24-18 Higashikoiwa, Edogawaku, Tokyo, 133-0052, Japan.
E-mail addresses: inokuchi1122@gmail.com (Y. Inokuchi), RI@edogawa.or.jp (M. Uematsu), navos70ho@yahoo.co.jp (T. Takashina).

https://doi.org/10.1016/j.ejro.2021.100347
Received 8 February 2021; Received in revised form 23 March 2021; Accepted 13 April 2021

into the hepatic ECS, the sinusoids are surrounded by thick fibrous tissue, the sinusoidal endothelium has a basement membrane, and the small pores shrink and disappear according to the increase in fibrous tissue. Such structural abnormalities caused decrease in the peripheral portal and hepatic vein perfusion [18–21]. This phenomenon leads to delayed hepatic enhancement in portal venous phase and delayed washing out of hepatic parenchymal contrast materials in the equilibrium phase in patients with cirrhosis [17,18,22–24]. Therefore, we considered that changes in intrahepatic hemodynamics owing to fibrosis could be evaluated with higher accuracy using the attenuation value (obtained by subtracting the CT value obtained from ADCE-MDCT imaging of the equilibrium phase from the value obtained from that of the portal phase in hepatic parenchyma) because we considered that the transition in hepatic enhancement represents the change in intrahepatic hemodynamics due to fibrosis.

Hence, this study aimed to investigate whether the attenuation value is useful in distinguishing normal liver tissues from LC and eventual future development of EVs in patients with LC.

2. Materials and methods

2.1. Patients

This study was approved by the relevant institutional review board, and the need to obtain informed consent from patients was waived owing to the retrospective nature of the study. We retrospectively recruited radiology information system outpatients who underwent ADCE-MDCT for the diagnosis of abdominal disease between February 2016 and December 2017. The patients were classified into two groups: patients with normal liver (group A) and those diagnosed with LC (group B). Patients with LC had undergone endoscopy and analysis of biomarkers related to hepatic function at the same time as ADCE-MDCT for diagnosis of LC. Patients with LC were further divided into two subgroups: those without EVs (group a) and those with EVs (group b). Group b included one patient with paraumbilical vein shunt and gastric vein varices, one with paraumbilical vein shunt, one with splenic vein varices and left ovarian vein varices, and one with gastric vein varices. LC was diagnosed based on clinical data, laboratory test, and imaging performed by a clinician. We excluded factors that could affect the hepatic enhancement (Fig. 1).

2.2. Computed tomography examination

A 64-detector CT scanner (Revolution EVO; GE Healthcare, Chicago, IL, USA) with a fixed tube voltage of 120 kVp and an automatic tube current modulation program was used to acquire CT data. The CT parameters used were as follows: collimation, 0.625 mm; detector configuration, 64 × 0.625 mm; noise index, 13; pitch factor, 0.984:1; gantry rotation time 0.5 s. All transverse CT images were reconstructed from 5-mm thickness sections, with the intensity of the adaptive statistical iterative reconstruction set at 50 %. Scans were performed in the cephalocaudal direction, and all CT images were obtained from the top of the liver to bottom of the ischium.

2.3. Administration of contrast media

In the contrast phase, monitoring was set at the level of the left ventricle, and the region of interest (ROI) was placed in the aorta. The trigger threshold level was set at 150 Hounsfield units (HU). At 15 s after the trigger, the late arterial phase scan was started. Additionally, the portal phase scan was conducted 35 s after the late arterial phase using a real-time monitoring system (Smart Prep), and the equilibrium phase scan was conducted 90 s after the portal phase (Fig. 2). All patients were injected with nonionic iodinated contrast material containing a total of 600 mg iodine per kg of body weight [25,26]. Further, in order to eliminate the difference in contrast ability between individual patients, the injection time was fixed at 30 s using a power injector (Dual Shot GX; Nemoto Kyourindou, Tokyo, Japan) [27]. The solution was injected through a 20 gage plastic intravenous catheter inserted into the median antebrachial, basilic, cephalic, or radial vein.

2.4. Quantitative analysis

The CT value of hepatic parenchyma was measured as delta HU by selecting circular ROIs of approximately 2 cm^2 within three areas (S3, S7, and S8 on the porta hepatis cross section) (Fig. 3). The mean CT value of the three ROIs was calculated. Then, the mean CT value of the non-enhanced phase was subtracted from that of the portal and equilibrium phases. The attenuation value was calculated by subtracting the CT value of the equilibrium phase from that of the portal phase.

2.5. Statistical analysis

Differences in the attenuation value, CT value of the hepatic

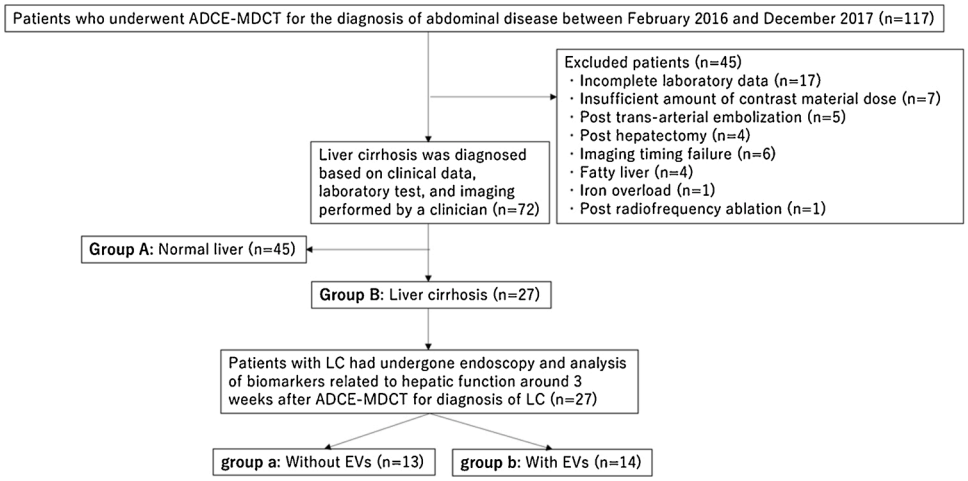

Fig. 1. Flow chart of patient enrollment.
ADCE MDCT abdominal contrast enhanced dynamic multi-detector-row computed tomography
LC liver cirrhosis
EVs esophageal varices.

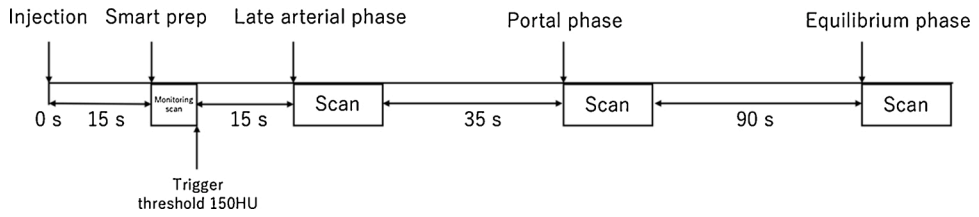

Fig. 2. Computed tomography scanning protocol.

Fig. 3. Position of ROIs for the measurement in contrast enhancement of hepatic parenchyma.
ROIs region of interests

parenchymal portal and CT value of the equilibrium phase were compared between groups A and B using the Student's *t*-test. We investigated the correlation between attenuation value and biomarkers related to hepatic function [serum albumin level, serum total bilirubin level, prothrombin activity, platelet count, fibrosis index based on the four factors (FIB-4), aspartate aminotransferase to platelet ratio index (APRI) and aspartate aminotransferase to alanine aminotransferase ratio (AAR)] using Pearson's correlation coefficient. We investigated differences in the attenuation value and biomarkers for the prediction of EVs (FIB-4, APRI and AAR) between the two subgroups of group B using the Student's *t*-test. To calculate the optimal cutoff value for the attenuation value, we performed receiver operating characteristic (ROC) analysis of FIB-4, APRI, and AAR for subgroup C vs D, and evaluated the diagnostic accuracy (sensitivity, specificity, positive predictive value, negative predictive value and area under the ROC curve [AUC]). Statistical significance was accepted at $P < .05$. All statistical analysis was performed using EZR software (Saitama Medical Center, Jichi Medical University, Saitama, Japan).

3. Results

The mean CT value for the hepatic parenchymal enhancement of the portal and equilibrium phases and the attenuation value were 58.0 HU ± 4.9 (range 49.3–65.9 HU), 36.2 HU ± 4.8 (range 27.9–48.2 HU) and 21.8 HU ± 5.2 (range 12.9–35.1 HU), respectively, for group A; 53.0 HU ± 6.1 (range 42.2–67.3 HU), 39.1 HU ± 5.5 (range 32.0–53.4 HU) and 13.8 HU ± 5.4 (range 2.1–25.3 HU), respectively, for group B; 56.9 HU ± 5.2 (range 51.1–60.5 HU), 38.8 HU ± 4.8 (range 32.05–48.1 HU), and 18.0 HU ± 3.2 (range 11.8–25.3 HU), respectively, for group a; and 49.7 HU ± 4.7 (range 42.2–59.3 HU), 39.3 HU ± 6.5 (range 32.2–53.4 HU) and 10.3 HU ± 3.9 (range 2.1–13.4 HU), respectively, for group b. The attenuation value and CT value for the hepatic parenchymal portal and equilibrium phase were significantly different ($P < 0.0001$, $P < 0.001$, and $P = 0.05$, respectively) between groups A and B (Fig. 3; Table 1).

The attenuation value was significantly different between groups a and b. The mean values of FIB-4, APRI, and AAR were higher in group b than group a, although this was not statistically significant (Table 2). The attenuation value was found to be correlated with serum albumin level, serum total bilirubin level, platelet count, FIB-4, and APRI in the group B (Table 3). For the prediction of EVs, the cutoff for attenuation value was found to be 13.4 HU (sensitivity, 92 %; specificity, 92 %; positive predictive value, 92 %; negative predictive value, 92 % and AUC, 0.954 [95 % confidence interval, 0.878–1]) according to ROC analysis. The cutoffs for FIB-4, APRI, and AAR were 6.8, 1.9, and 1.5 (sensitivity: 57 %, 57 %, and 64 %; specificity: 76 %, 84 %, and 79 %; positive predictive value: 70 %, 78 %, and 75 %; negative predictive value: 63 %, 66 %, and 68 % and AUC: 0.659, 0.665, and 0.646 [95 % confidence interval: 0.441–0.877, 0.45–0.88, and 0.423–0.868]), respectively (Fig. 4).

Table 1
Patient characteristics.

	A	B	P Value†
No. of patients	45	26	NA
Male : Female	37 : 18	9 : 17	NA
Age (y)*	69.1 ± 10.9	74.5 ± 5.7	0.024
eGFRcreat (mL/min/1.73 m^2) *	71.7 ± 17.1	76.6 ± 19.3	0.303
Etiology (HBV/HCV/Alcohol/Other)	NA	2/12/9/9	NA
Child-pugh classification (A/B/C)	NA	19/8/0	NA
Trigger time (s)	19.9 ± 3.2	19.5 ± 2.2	0.623
Time for the late arterial phase (s)	34.9 ± 3.2	34.5 ± 2.2	0.623
Time for the portal phase (s)	76.6 ± 3.2	76.4 ± 2.9	0.850
Time for the equilibrium phase (s)	173.3 ± 3.5	173.9 ± 3.9	0.948

eGFRcreat estimated glomerular filtration rate from serum creatine levels.
* Data are mean ± standard deviation, with range in parentheses.
† P value was obtained with the Student's *t*-test.

Table 2
Patient characteristics of two subgroups in group B.

	a (without EVs) n = 13	b (with EVs) n = 14	P Value†
Male : Female	9 : 4	5 : 9	NA
Age (y)*	76.1 ± 5.4	73.0 ± 5.8	0.167
Serum albumin levels (g/dl)	4.00 ± 0.48	3.56 ± 0.43	0.025
Serum total bilirubin level (ml/g)	0.91 ± 0.35	1.25 ± 0.47	0.054
Platelet count (10^3/μl)	125.61 ± 47.44	98.84 ± 48.23	0.167
FIB-4	5.76 ± 3.27	9.75 ± 7.08	0.077
APRI	1.34 ± 0.89	2.49 ± 1.78	0.049
AAR	1.38 ± 0.47	1.66 ± 0.84	0.307
Attenuation value (HU)	18.0 ± 3.2	10.4 ± 4.4	< 0.001
eGFRcreat (mL/min/1.73 m^2) *	71.6 ± 19.6	81.5 ± 18.4	0.2
Etiology (HBV/HCV/Alcohol/Other)	1/7/3/2	1/4/1/8	NA
Child-pugh classification (A/B/C)	11/2/0	8/6/0	NA

Data are mean ± standard deviation, with range in parentheses.
eGFRcreat estimated glomerular filtration rate from serum creatine levels.
FIB-4 fibrosis index based on the four factors.
APRI aspartate aminotransferase to platelet ratio index.
AAR aspartate aminotransferase to alanine aminotransferase ratio.
† P value was obtained with the Student's *t*-test.

Table 3
Correlation between the attenuation value and biomarkers in group B.

	Correlation coefficient	95 %CI	P Value†
Serum albumin levels (g/dl)	0.302	0.0756–0.499	0.00993
Serum total bilirubin level (ml/g)	−0.516	−0.668 to −0.357	< 0.00001
Platelet count (10^3/μl)	0.459	0.255–0.625	< 0.00001
FIB-4	−0.544	−0.698 to −0.356	< 0.00001
APRI	−0.582	−0.717 to −0.405	< 0.00001
AAR	−0.138	−0.359 to −0.0964	0.246

CI confidence interval.
FIB-4 fibrosis index based on the four factors.
APRI aspartate aminotransferase to platelet ratio index.
AAR aspartate aminotransferase to alanine aminotransferase ratio.
† P value was obtained with the Pearson's correlation coefficient.

4. Discussion

The present study focused on changes in the intrahepatic hemodynamics according to hepatic fibrosis among patients with LC. We investigated these changes be evaluating the changes in hepatic enhancement between portal and equilibrium phase to evaluate the potential clinical utility of the attenuation value. Our study found that patients with cirrhosis had decreased hepatic enhancement in portal venous phase and slightly increased hepatic enhancement in equilibrium phase when compared with those who had normal liver, this was similar to the observations reported in several previous studies [17,18,22–24]. In the attenuation value, between LC patients and normal liver patients more significant difference was observed. Namely, the attenuation value indicates the hemodynamics change in intrahepatic contrast material due to an increase in intrahepatic vessel resistance by hepatic fibrosis, and the study suggested that this parameter reflects the characteristics from inflow to out flow of the contrast material during the portal and equilibrium phases (Fig. 5). Additionally, the correlation of attenuation value with major biomarkers related to hepatic fibrosis supports the utility of attenuation value in this capacity. We discovered that the attenuation value may represent a new indicator for the quantitative classification of normal liver and LC.

We considered that the attenuation value may have utility for predicting EVs considering the current opinion regarding the mechanism of EV development [4,9,28]. Naruo et al. reported that hepatic enhancement of portal phase was remarkably decreased by cirrhosis patients with a portosystemic shunt [29]. Our results are similar; comparison of data from patients with and without EVs revealed that the attenuation value and hepatic enhancement of portal phase were significantly different according to the presence or absence of EVs, and thus may have utility in the prediction or diagnosis of this condition. We also found the cutoff value to separate the LC patients with EVs. Several previous studies have revealed that FIB-4, APRI, and AAR are biomarkers of hepatic fibrosis and can be evaluated for the prediction of EVs, and these markers exhibit significant differences between patients with LC with and without EVs [30–32]. We only identified a significant difference in the attenuation value of patients with LC when those with and without EVs were compared. Furthermore, we found the AUC, sensitivity and specificity of biomarkers to be in line with the results of a meta-analysis performed by Han et al. [31], suggesting that our patient data were suitable for the present. Taken together, the results of the present and previous studies described above suggest that the prediction of EVs by evaluation of the attenuation value is a valid, non-invasive approach which is superior in terms of AUC, sensitivity, and specificity to analysis of FIB-4, APRI, and AAR. To date, the degree of hepatic fibrosis in imaging examination requires the use of special devices accompanying magnetic resonance imaging and ultrasonography [33,34]. Further, MDCT should be performed in combination with biochemical test [35]. Furthermore, to the best of our knowledge, predicting the development of EVs at imaging examination has not been reported. The attenuation value can be analyzed retrospectively from ADCE-MDCT data, thereby eliminating the requirement for additional examinations. Thus, we suggest that the occurrence of hepatocellular carcinoma, changes in gross morphology of the liver, the presence or absence of EVs, and the predictor of EVs in patients with LC is possible using ADCE-MDCT data from a single examination. We may that this information can improve the quality of care and medical costs for patients with LC in terms of risk management in MDCT.

This study has some limitations which should be acknowledged. Firstly, the assessment of fibrosis in attenuation values was compared with only blood test data. Therefore, it is necessary to compare the changes in liver fibrosis at attenuation values with elastography and liver biopsy data in the future. Secondly, the CT value that was taken as the attenuation value is known to vary between different CT devices [16]. So, the attenuation value is likely to slightly fluctuate according to the specific equipment. Finally, the number of cases of LC was low in this study. Therefore, we considered that not obtaining significant

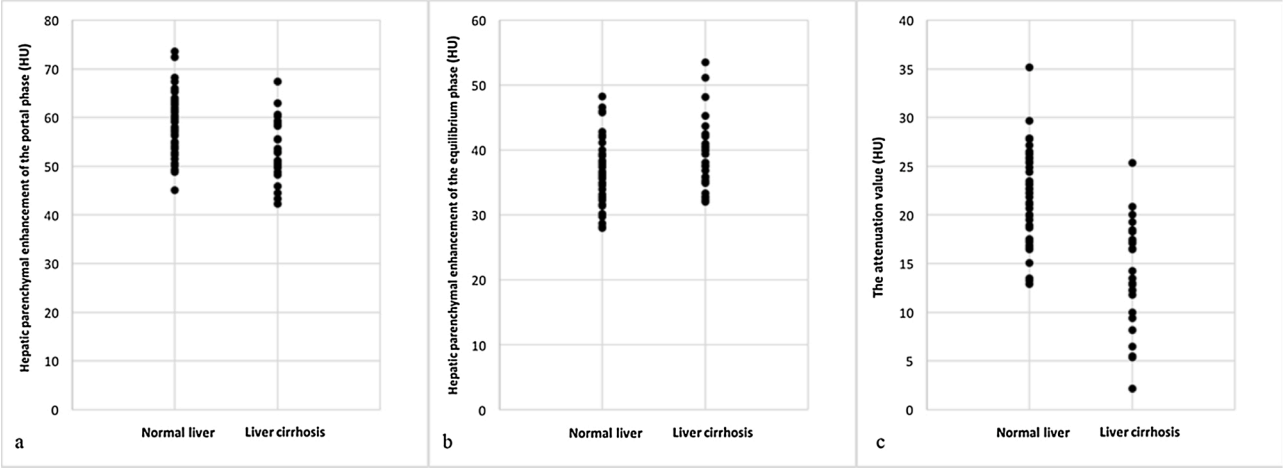

Fig. 4. Dot-plot shows the relationship between group A and B. (a) Hepatic parenchymal enhancement of the portal phase: Student's *t*-test $P < 0.001$ (b) Hepatic parenchymal enhancement of the equilibrium phase: Student's *t*-test $P = 0.05$. (c) The attenuation value: Student's *t*-test $P < 0.0001$. Significant differences were obtained all items.

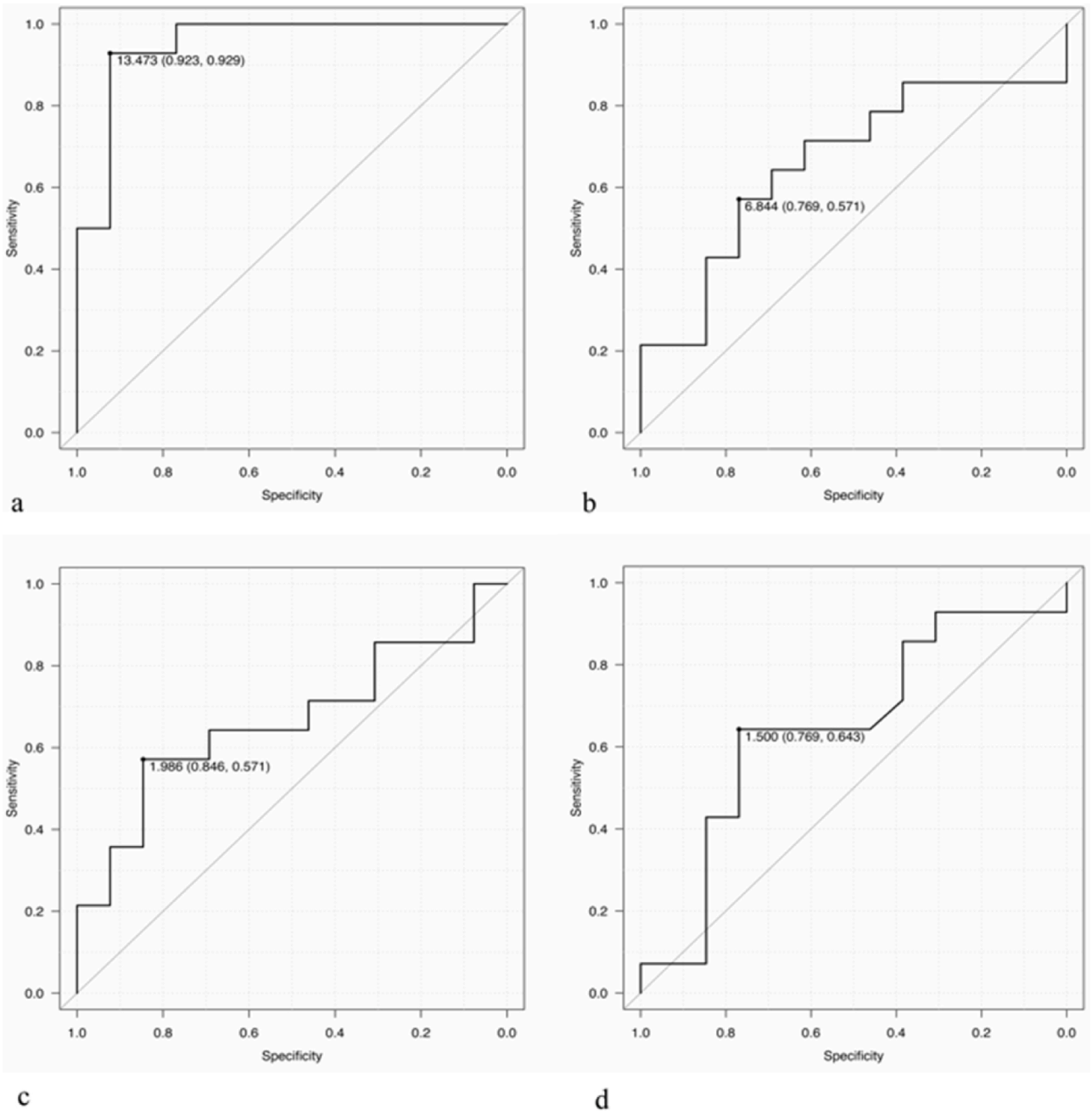

Fig. 5. Graph show ROC curve for separating subgroup a and b. (a) The attenuation value: The optimal cut-off value of the attenuation value was 13.4HU. (b) FIB-4: The optimal cut-off value of FIB-4 was 6.8. (c) APRI: The optimal cut-off value of APRI was 1.9. (d) AAR: The optimal cut-off value of AAR was 1.5.

differences between FIB-4, APRI, and AAR in patients with and without EVs as a factor. Thus, future studies should include more number of patients.

In conclusion, the attenuation value obtained by subtracting the CT value of the equilibrium phase from that of the portal phase for the hepatic parenchyma from ADCE-MDCT appears to have utility for the classification of normal liver and LC and the prediction of EVs in patients with LC.

Author contributions

1, guarantor of integrity of the entire study: Tsuneyuki Takashina
2, study concepts and design: Yasuhiro Inokuchi
3, literature research: Yasuhiro Inokuchi, Tsuneyuki Takashina
4, clinical studies: Yasuhiro Inokuchi, Masahiro Uematsu, Tsuneyuki Takashina
5, experimental studies / data analysis: Yasuhiro Inokuchi, Tsuneyuki Takashina
6, statistical analysis: Yasuhiro Inokuchi, Tsuneyuki Takashina
7, manuscript preparation: Yasuhiro Inokuchi, Tsuneyuki Takashina
8, manuscript editing: Yasuhiro Inokuchi, Tsuneyuki Takashina

Funding statement

The authors state that this work has not received any funding.

Ethical statement

Institutional Review Board approval was obtained.

Declaration of Competing Interest

This research did not receive any specific grant from funding agencies in the public, commercial, or not-for-profit sectors. The authors declare that they have no conflict of interest.

References

[1] K.C. Sudhamshu, Shoiichi Matsutani, Hitoshi Maruyama, Taro Akiike, Hiromitsu Saisho, Doppler study of hepatic vein cirrhotic patients: correlation with liver dysfunction and hepatic hemodynamics, World J. Gastroenterol. 12 (36) (2006) 5853–5858.
[2] P. Gines, G. Fernandez-Esparrach, V. Arroyo, Ascites and renal functional abnormalities in cirrhosis: pathogenesis and treatment, Baillieres Clin. Gastroenterol. 11 (2) (1997) 365–385.
[3] Francesco Salerno, Monica Guevara, Mauro Bernardi, Richard Moreau, Florence Wong, Paolo Angeli, Refractory ascites: pathogenesis, definition and therapy of a severe complication in patients with cirrhosis, Liver Int. 30 (8) (2010) 937–947.
[4] J. Bosch, P. Pizcueta, F. Feu, M. Fernández, J.C. García-Pagán, Pathophysiology of portal hypertension, Gastroenterol. Clin. North Am. 21 (1) (1992) 1–14.
[5] Roberto de Franchis, Baveno V. Faculty, Revising consensus in portal hypertension: report of the Baveno V consensus workshop on methodology of diagnosis and therapy in portal hypertension, J. Hepatol. (53) (2010) 762–768.
[6] B.M. Spiegel, L. Targownik, G.S. Dulai, H.A. Karsan, I.M. Gralnek, Endoscopic screening for esophageal varices in cirrhosis: is it ever cost effective? Hepatology 37 (2) (2003) 366–377.
[7] J.A. Talwalkar, P.S. Kamath, Screening for esophageal varices among patients with cirrhosis of the liver, Am. J. Gastroenterol. 96 (10) (2001) 3039–3040.
[8] S. Bloom, W. Kemp, J. Lubel, Portal hypertension: pathophysiology, diagnosis and management, Intern. Med. J. 45 (1) (2015) 45, 16–26.
[9] Y. Iwakiri, Rj Groszmann, The hyperdynamic circulation of chronic liver diseases: from the patient to the molecule, Hepatology 43 (2 Suppl. 1) (2006) 121–131.
[10] M.J.K. Blomely, A.K.P. Lim, C.J. Harvey, N. Patel, R.J. Eckersley, R. Basilico, et al., Liver microbubble transit time compared with histology and Child-Pugh score in diffuse liver disease: a cross sectional study, Gut 52 (8) (2003) 1188–1193.
[11] T. Albrecht, M.J. Blomley, D.O. Cosgrove, S.D. Taylor-Robinson, V. Jayaram, R. Eckersley, et al., Non-invasive diagnosis of hepatic cirrhosis by transit-time analysis of an ultrasound contrast agent, Lancet 353 (9164) (1999) 1579–1583.
[12] Woo Kyoung Jeong, Tae Yeob Kim, Joo Hyun Sohn, Yongsoo Kim, Jinoo Kim, Severe portal hypertension in cirrhosis: evaluation of perfusion parameters with contrast enhanced ultrasonography, PLoS One 10 (3) (2015) 1–14.
[13] Hiroyuki Akai, Shigeru Kiryu, Izuru Matsuda, Jirou Satou, Hidemasa Takao, Taku Tajima, et al., Detection of hepatocellular carcinoma by Gd-EOB-DTPA-enhanced liver MRI: comparison with triple phase 64 detector row helical CT, Eur. J. Radiol. 80 (2) (2011) 310–315.
[14] H. Deng, X. Qi, X. Guo, Computed tomography for the diagnosis of varices in liver cirrhosis: a systematic review and meta-analysis of observational studies, Postgrad. Med. 129 (3) (2017) 318–328.
[15] M. Hori, T. Okada, K. Higashiura, Y. Sato, Y.-W. Chen, T. Kim, et al., Quantitative imaging: quantification of liver shape on CT using the statistical shape model to evaluate hepatic fibrosis, Acad. Radiol. 22 (3) (2015) 303–309.
[16] K. Awai, S. Date, Basic knowledge to achieve optimal enhancement of CT, Nichidoku-Iho 56 (1) (2011) 13–32.
[17] K.T. Bae, Intravenous contrast medium administration and scan timing at CT: considerations and approaches, Radiology 256 (1) (2010) 32–61.
[18] O. Vignaux, P. Legmann, J. Coste, C. Hoeffel, A. Bonnin, Cirrhotic liver enhancement on dual-phase helical CT: comparison with noncirrhotic livers in 146 patients, AJR Am. J. Roentgenol. 173 (5) (1999) 1193–1197.
[19] Y. Soroida, T. Nakatsuka, M. Sato, H. Nakagawa, M. Tanaka, N. Yamauchi, et al., A novel non-invasive method for predicting liver fibrosis by quantifying the hepatic vein waveform, J. Ultrasound Med. Biol. 45 (9) (2019) 2363–2371.
[20] N. Berndt, M.S. Horger, S. Bulik, H.-G. Holzhütter, A multiscale modelling approach to assess the impact of metabolic zonation and microperfusion on the hepatic carbohydrate metabolism, PLoS Comput. Biol. 14 (2) (2018), e1006005.
[21] M. Bolognesi, A. Verardo, M.D. Pascoli, Peculiar characteristics of portal-hepatic hemodynamics of alcoholic cirrhosis, World J. Gastroenterol. 220 (25) (2014) 8005–8010.
[22] O. Vignaux, H. Gouya, J. Augui, A. Oudjit, J. Coste, B. Dousset, et al., Hepatofugal portal flow in advanced liver cirrhosis with spontaneous portosystemic shunts: effects on parenchymal hepatic enhancement at dual-phase helical CT, Abdom. Imaging 27 (2002) 536–540.
[23] V. Varenika, Yanjun Fu, Jacquelyn J. Maher, Dongwei Gao, Sanjay Kakar, Miguel C. Cabarrus, et al., Hepatic fibrosis: evaluation with semiquantitative contrast-enhanced CT, Radiology 266 (1) (2013) 151–158.
[24] S. Bandula, S. Punwani, W.M. Rosenberg, R. Jalan, A.R. Hall, A. Dhillon, et al., Equilibrium contrast-enhanced CT imaging to evaluate hepatic fibrosis: initial validation by comparison with histopathologic sampling, Radiology 275 (1) (2015) 136–143.
[25] Y. Yamashita, Y. Komohara, M. Takahashi, M. Uchida, N. Hayabuchi, T. Shimizu, et al., Abdominal helical CT: evaluation of optimal doses of intravenous contrast material a prospective randomized study, Radiology 216 (3) (2000) 718–723.
[26] K. Awai, S. Hori, Effect of contrast injection protocol with dose tailored to patient weight and fixed injection duration on aortic and hepatic enhancement at multidetector-row helical CT, Eur. Radiol. 13 (9) (2003) 2155–2160.
[27] T. Ichikawa, Sukru Mehment Erturk, T. Araki, Multiphasic contrast-enhanced multidetector-row CT of liver: contrast-enhancement theory and practical scan protocol with a combination of fixed injection duration and patients' body-weight-tailored dose of contrast material, Eur. J. Radiol. 58 (2) (2006) 165–176.
[28] A.K. Pillai, B. Andring, A. Patel, C. Trimmer, S.P. Kalva, Portal hypertension: a review of portosystemic collateral pathways and endovascular interventions, Clin. Radiol. 70 (10) (2015) 1047–1059.
[29] K. Naruo, M. Tozaki, Y. Fukuda, K. Fukuda, Enhancement of the liver on dynamic MDCT: investigation among three groups consisting of noncirrhotic patients and cirrhotic patients with and without a large portosystemic shunt, Radiat. Med. 25 (3) (2007) 106–112.
[30] Y. Sumida, M. Yoneda, H. Hyogo, Y. Itoh, M. Ono, H. Fujii, et al., Validation of the FIB4 in a Japanese nonalcoholic fatty liver disease population, BMC Gastroenterol. 5 (12:2) (2012).
[31] D. Han, Q. Xingshun, G. Xiaozhong, Diagnostic accuracy of APRI, AAR, FIB-4, FI, king, lok, forns, and FibroIndex scores in predicting the presence of esophageal varices in liver cirrhosis: a systematic review and meta-analysis, Medicine (Baltimore) 94 (42) (2015) e1795.
[32] K. Bledar, M. Iris, A. Ilir, K. Adea, P. Skerdi, B. Genc, Predictors of esophageal varices and first variceal bleeding in liver cirrhosis patients, World J. Gastroenterol. 23 (26) (2015) 4806–4814.
[33] S. Hoodeshenas, M. Yin, S.K. Venkatesh, Magnetic resonance elastography of liver: current update, Top. Magn. Reson. Imaging 27 (5) (2018) 319–333.
[34] E.A. Tsochatzis, K.S. Gurusamy, S. Ntaoula, E. Cholongitas, B.R. Davidson, A. K. Burroughs, Elastography for the diagnosis of severity of fibrosis in chronic liver disease: a meta-analysis of diagnostic accuracy, J. Hepatol. 54 (4) (2011) 650–659.
[35] Y. Shinagawa, K. Sakamoto, K. Sato, E. Ito, H. Urakawa, K. Yoshimitsu, Usefulness of new subtraction algorithm in estimating degree of liver fibrosis by calculating extracellular volume fraction obtained from routine liver CT protocol equilibrium phase data: preliminary experience, Eur. J. Radiol. 103 (2018) 99–104.